PROCEEDINGS OF SPIE

Real-time 3D video moire inspection system with enhanced depth resolution

Donald W.W. Dawson
Chris L. Hart
Bernard R. Gilbert
Gary L. Wallace
Joel H. Blatt

SPIE.

Real time 3-D video moiré inspection system with enhanced depth resolution

Donald W.W. Dawson, MEMBER SPIE
Chris Hart
Bernard Gilbert III
Gary L. Wallace*
Joel H. Blatt (blatt@pss.fit.edu), MEMBER SPIE

Florida Institute of Technology, Physics and Space Sciences Department
150 West University Boulevard, Melbourne, FL 32901-6988

ABSTRACT

A variable resolution video machine vision system has been built which generates twice the number of depth contours for a given grating spacing as a conventional moiré system. This variable resolution system uses a Mach-Zender interferometer to project interference fringes onto a reference surface and onto a target surface. Video images of the two structurally illuminated surfaces are mixed in a video mixer with the resulting output being moiré contours which are the intersections of the two surfaces. If the reference surface is a flat plate, we get equal depth contours of the target surface, and if the reference surface is a perfect target, we get error map contours of the 3-D shape differences between the two targets. Theoretical analysis has shown that if the reference surface upon which the gratings are projected is the inside (inverse) of the actual surface to be inspected, then the moiré depth contours are twice as dense as would be observed with a flat reference surface. This surprising result is experimentally demonstrated both for a perfect target and for a target with 3-D shape errors. Real time error maps of damaged targets made using this technique have many Moiré contours outside the area of interest, but this "non information" can be greatly reduced by video or computer subtraction of the perfect target images. Limitations and improvements in the current system will be discussed.

Key Words: Moiré contouring, 3-D inspection, video inspection

1. INTRODUCTION

We have developed a variable resolution video moiré machine vision system that allows the generation of some highly unusual moiré contours. In a conventional projection moiré system, a fixed spacing physical grating is used to project structured illumination onto a 3-D target. A camera views the distorted illumination through a matched grating in an intermediate focal plane, generating equal depth moiré contours as a low frequency interference pattern superimposed on the images of the distorted structured illumination and the intermediate grating. In our system, the structured illumination is generated by a laser illuminated tilted mirror interferometer, allowing us to vary the spatial frequency by changing the mirror tilt[1]. The lack of a physical reference grating means that some other means must be used to generate the moiré beat pattern. We split the beam from the interferometer and project it onto two surfaces, the target surface, and a reference surface, as shown in Fig. 1. Video cameras view the two surfaces, and the images are combined in a video mixer to generate the moiré contours[2]. The resulting mixed image is sent to a frame grabber. The fact that there is a physical reference surface intimately connected with the shape of the moiré contours allows some unusual applications. If the reference surface is a flat plate, the video mix produces conventional equal depth moiré contours. If, however, the reference surface is a perfect version of the target, moiré error maps are seen, representing depth contours of the differences between the targets[3,4]. If two different surfaces are used the moiré contours represent the family of intersections of the two surfaces[5]. In this paper, we consider the consequences when the reference surface is the inverse of the target surface, and we show theoretically and experimentally that twice as many contours are produced using the inverse target as a reference surface as compared to a flat plate reference surface.

---

* Current address: 3625 Misty Oak Drive #303, Melbourne, FL 32901

2. THEORY

Consider an arbitrary surface z=f(x,y) which is illuminated by projected gratings of pitch P, with the gratings appearing as lines in the y-z plane. We index the lines by an integer m, which is taken as zero for the line passing through the origin. The equation of the projected gratings can be written as $z_m = y[\cot(\alpha)] - mP[\csc(\alpha)]$. When this equation is intersected with the equation describing the surface one gets the form of the distorted projected gratings. Next consider two surfaces z_1 and z_2 with $z_2 = \delta z_1$ where δ is any real constant. If we intersect each surface with the projected gratings, we get

$$z_1[\sin(\alpha)] = y[\cos(\alpha)] - mP \tag{1}$$

$$z_2[\sin(\alpha)] = y[\cos(\alpha)] - nP = \delta z_1[\sin(\alpha)] . \tag{2}$$

To get the low frequency moiré we subtract equation (2) from equation (1) to get

$$(n - m)P = (1 - \delta)z_1[\sin(\alpha)]. \tag{3}$$

Let the integer $I = n - m$. In the case of a flat reference surface, $\delta = 0$ and we get

$$IP = z_1[\sin(\alpha)], \tag{4}$$

the equation of equal depth contours of the target surface z_1. If $\delta = 1$ the two surfaces are identical and we get IP = 0 (no moiré contours). The case we are interested in here, is when $\delta = -1$, which corresponds to z_2 being the inverse surface to z_1 (i.e., if z_1 was a cone then z_2 would be would be a cone shaped hole that the cone could fit into, or in other words, $z_1 + z_2 = 0$, a flat surface). We then find that the equation for the moiré fringes is

$$IP = 2z_1[\sin(\alpha)] \quad \text{or} \quad IP/2 = z_1[\sin(\alpha)], \tag{5}$$

again equal depth contours, but now we get twice as many moiré fringes as we got with the flat reference surface - i.e., the cross sections of the moiré surface in equation (4) are taken at intervals of IP/2 instead of at intervals of IP as before[6]. Other choices are possible, for instance if $\delta = -2$, our reference surface is an inverse of a target that is twice as steep as the target. We now get 4 times as many contours (i.e., the contours occur at IP/4). If we choose $\delta = +2$, then our reference surface is twice as steep as the original target, but $(1 - \delta) = -1$ and we get the surprising result that the contours are identical in spacing (but shifted) when compared to those obtained with a flat plate reference surface ($\delta = 0$) and $(1 - \delta) = +1$.

3. EXPERIMENTAL SETUP

We use an Ar-Ion laser to illuminate a Michelson or Mach-Zender interferometer set up with one mirror tilted off axis, allowing us to vary the spatial frequency of the projected fringes by adjusting the mirror tilt. If the Michelson is used, a lens system eliminates the beam steering caused by the mirror tilt[6,7], and a beamsplitter generates the target and reference beams as shown in Fig. 1. When a Mach-Zender is used, neither projection optics nor a beamsplitter are needed. The video cameras are each equipped with macro zoom lenses allowing matching of the scale of the target and reference images. The video signals are sent to a JVC KM-1200 color video special effects generator (mixer) where the reference signal is used to chroma-key the target signal, generating the low frequency moiré interference. A small amount of the reference signal is fed back to improve the signal to noise ratio[2]. A Macintosh IICi captures the images using a Data Translation Quick Capture frame grabber board. A piezoelectric driver is used to translate one of the mirrors to give precise control of the fringe location and also to allow for further signal-to-noise enhancement of the moiré fringes using the frame average feature of the image processing software, NIH Image. A Scion TV-3 video output board allows NIH Image to output computer generated or computer processed images back to the mixer, where they can be mixed with live video.

4. EXPERIMENTAL RESULTS

In order to verify the theory starting with a simple 3-D geometry, an aluminum cone was chosen as the first target (base diameter 5.08 cm and 2.54 cm height). A video image of the cone is shown in Fig. 2, with a set of "normal" equal depth moiré contours shown in Fig. 3a. These contours were obtained in real time when the reference surface was a flat plate ($\delta = 0$). An inverse surface ($\delta = -1$) was then made up by pressing modeling clay over the cone and using the indentation as the reference surface. Fig. 3b shows the moiré contours of the cone in this case. Comparing Figs. 3a and 3b the doubled depth resolution of the contours can be easily seen. If a new reference surface is made as the inverse of a cone twice as steep as the original ($\delta = -2$), we get 4 times the number of contours, as seen in Fig. 3c. If we use the 2x steep cone as a reference ($\delta = +2$), we see in Fig. 3d the same set of contours as with the flat plate reference (Fig. 3a), but shifted ($1 - \delta = +1$ for the flat plate and $1 - \delta = -1$ for the 2x cone).

Next a dented pipe (4.45 cm diameter by 12.7 cm long with 0.82 cm deep dent) was chosen as a more interesting target, as shown in Fig. 4a. Fig. 5a shows the normal equal depth contours (flat plate reference, $\delta = 0$) while Fig. 5b shows the error maps generated when the reference surface is a perfect pipe ($\delta = +1$, except the dent is not present). As one would predict, the pipe itself shows no contours (unless it is misaligned relative to the reference pipe), but the dent contours show up clearly. This technique should be useful in manufacturing inspection since there is a considerable reduction in non useful information (the known shape of the pipe) and subsequent enhancement of important information (the contours of the dent). As mentioned before, a slight modification of this technique can indicate bends, kinks, or misalignment in continuously manufactured objects[3]. Next (Fig. 4b) we prepared a reference surface that was a perfect pipe ($\delta = +1$ for the pipe) to which we added a protruding piece of clay (dimple) molded into the inverse of the dent ($\delta = -1$ for the dent). In Fig. 5c we see the result of having our reference surface the perfect pipe but with the inverse dent, doubling the number of dent contours while having no contours on the pipe itself.

5. CONCLUSIONS

By choosing a particular reference surfaces, we have demonstrated that an arbitrary number of equal depth moiré contours can be generated when inspecting known surfaces through our video moiré technique. When looking for specific errors in industrial inspection, a choice of a reference surface which is identical to a perfect target surface combined with the inverse surface of the error shows great promise. The advantage is reduction in unwanted information (the contours of the "good part" of the target) and the enhancement of desired information (the enhanced contours of the error surface). If the error surface is not identical to the reference (inverse) error, there will still be an enhanced number of contours, though they will generally not be equal depth contours. As we have shown in previous work[8], it is possible to generate arbitrary moiré contours by computer generating a custom shaped reference surface and converting that image into RS-170 (composite) video. Thus the reference surface could be dynamically changed to "sweep" for imperfections on the target or could sweep at increasing quality levels. An additional degree of freedom can be realized by making the projection illumination pattern arbitrary[9], and these techniques can be combined to make to allow real-time optical processing for target detection and recognition[10]. In summary, this research could lead to the development of practical moiré based 3-D inspection techniques with enhanced useful information, enhanced depth resolution, and most important, enhanced defect detection.

6. REFERENCES

1. J. H. Blatt, R.V. Belfatto, J. A. Hooker and E.H. Young, "Video Applications to Moiré Metrology" Journal of Laser Applications, Vol. 2, No. 3 & 4, 35, Summer/Fall 1990.
2. J.H. Blatt, J.A. Hooker, H.-C. C. Ho, and E. H. Young, "The application of acousto-optic cells and video processing to achieve signal-to-noise improvements in variable resolution moiré profilometry", Optical Engineering 31(10), 2129-2138, (1992).
3. J.H. Blatt, S.C. Cahall, and J.A. Hooker, "Variable Resolution Video Moiré Error Map System For Inspection Of Continuously Manufactured Objects", SPIE Proceedings Vol. 1821, Industrial Applications of Optical Inspection, Metrology, and Sensing, 296-303 (1992).
4. B.G. Grossman, F.S. Gonzalez, J.H. Blatt, and S.C. Cahall, "Detection And Location Of Pipe Damage By Artificial Neural Net Processed Moiré Error Maps", SPIE Proceedings Vol. 1821, Industrial Applications of Optical Inspection, Metrology, and Sensing, 415-427 (1992).

46

5. S.C. Cahall, J.A. Hooker, and J.H. Blatt, "Real-Time Generation Of Intersection Of Surfaces For Welding By Video Moiré", SPIE Proceedings Vol. 2066, Industrial Optical Sensing and Metrology: Applications and Integration, 86-97 (1993).

6. J.A. Hooker, "Video Applications to Moiré Metrology", Ph.D. Dissertation, Florida Institute of Technology, 97-98, (1991).

7. J.H. Blatt, J.A. Hooker, and F.M. Caimi, "Adaptation Of Video Moiré Techniques To Under Sea Mapping And Surface Shape Determination", Optics and Lasers in Engineering, 16, issues 4 & 5, 265-278, 1992.

8. B.S. Gilbert III and Joel Blatt, "Generation of Arbitrary Moiré Contours for Automated Inspection", SPIE Proceedings Vol. 2065, Optics, Illumination, and Image Sensing for Machine Vision VIII, 144-150 (1993).

9. Scott C. Cahall, Bernard S. Gilbert III, and Joel H. Blatt, "Design of Arbitrary Projection Patterns for Object Recognition", SPIE Proceedings Vol. 2348, Imaging and Illumination for Metrology and Inspection, 34-45 (1994).

10. Rafael A. Andrade, Bernard S. Gilbert III, Donald W.W. Dawson, Samuel P. Kozatis, and Joel H. Blatt, "Real-time optically processed face recognition system based on arbitrary moiré contours", Optical Engineering 35(9), 2534-2540, (1996).
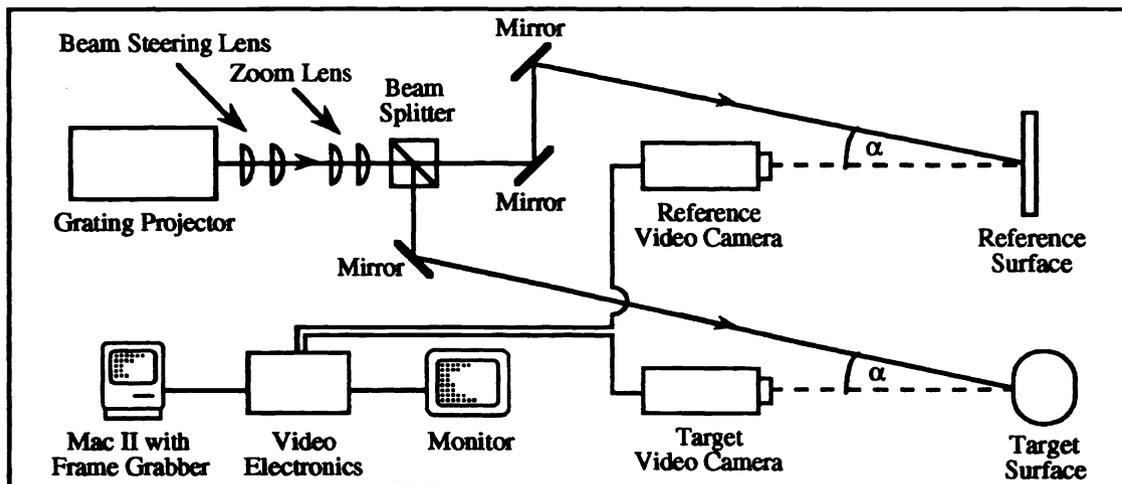
7. FIGURES

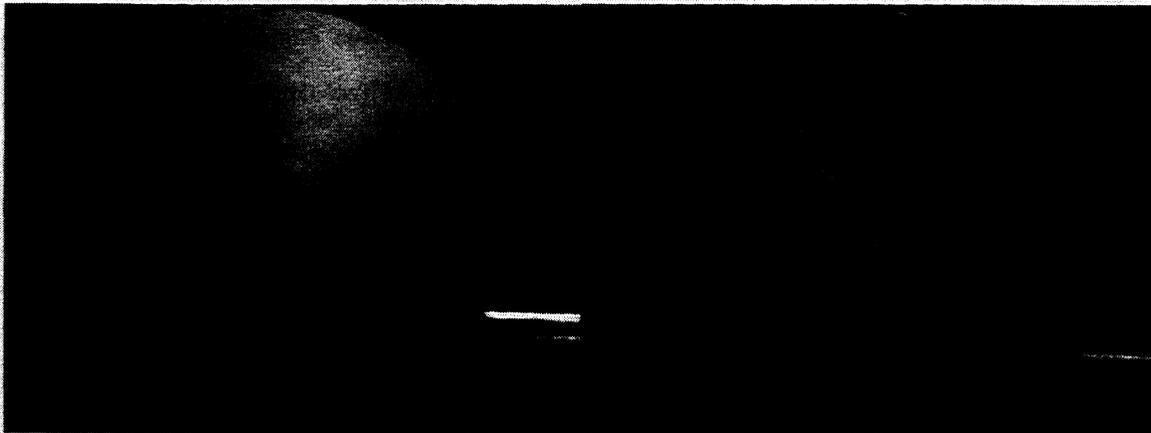Figure 1: Variable resolution video moiré setup.

Figure 2. Cone image

Figure 3a. Flat plate reference surface:
Equal depth contours of cone

Figure 3b. Inverse surface:
Equal depth contours of cone at double density

Figure 3c. Inverse surface twice as steep:
Equal depth contours of cone at 4x density

Figure 3d. Twice as steep surface:
Equal depth contours of cone

48

Figure 4a. Image of pipe with dent

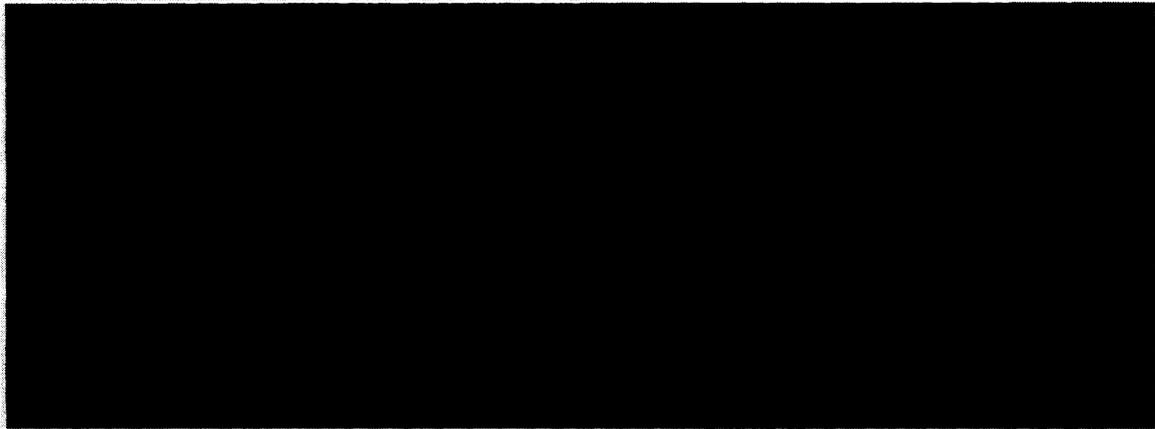Figure 4b. Image of pipe with dimple

Figure 5a. Flat plane reference surface:
Equal depth contours of dented pipe

Figure 5b. Perfect surface as reference:
Error map contours of dent

Figure 5c. Perfect surface plus inverse dent as reference:
Double density contours of dent

49